High Bypass Turbofan Engine Performance: Intake Pressure Recovery Effect

E. S. Abdelghany
Mechanical Engineering Departement.
Faculty of Engineering, Al-Baha University, KSA, on Leave from
Institute of Aviation Engineering and Technology, Giza, Egypt
eslam@bu.edu.sa

***Abstract*— The aviation industry continues to innovate onboard systems to enhance efficiency. This research examines the role of engine intake performance, specifically pressure recovery (PR), in improving the performance of a three-spool turbofan engine. Variations in an aircraft's flight path have a direct impact on pressure recovery. A computational fluid dynamics (CFD) model was first developed to assess pressure recovery at various angles of attack (0°, 10°, 20°, 30°, and 40°) at a Mach number of 0.82 and an altitude of 12,000 meters. Using ANSYS FLUENT® 19 with the Spalart-Allmaras turbulence model, the simulations revealed that the pressure recovery is highest at lower angles and gradually decreases at higher angles, with values between 0.92 and 0.98. MATLAB was then employed to analyze how intake pressure recovery affects the performance of a three-spool turbofan engine under similar conditions, with a Mach number range from 0.2 to 1. The results showed that improved pressure recovery led to a 4% enhancement in specific thrust, a 3% reduction in thrust-specific fuel consumption, and overall gains in engine efficiency. The study suggests that maintaining high pressure recovery is crucial to optimizing engine performance.**

Keywords*— *Turbofan Engine, Jet Engine Performance, Jet Engine Intake Efficiency, Pressure Recovery, CFD, thermodynamic cycle.

I.INTRODUCTION

With the anticipated rapid expansion of air travel, it is crucial for policymakers, as well as aircraft and engine manufacturers, to consider both the economic and environmental implications associated with the industry, [1]. The primary goal in developing new aircraft engines is to increase overall efficiency, with a focus on optimizing intake performance, [2]. The aircraft engine intake is a critical element that affects both propulsion and the aerodynamic aircraft performance, [3]. The engine intake provides the necessary free-streaming air into the engine by reducing the flow's velocity and converting its kinetic energy into pressure. Throughout different flight phases, varying in speed from subsonic to supersonic, the intake essential deliver adequate airflow to the engine. While it doesn't directly influence the airflow, it plays a crucial role in ensuring the air quality at the compressor inlet, requiring high total pressure and minimal distortion, [4]. The placement and design of the inlet significantly influence the aerodynamic forces on the aircraft, as it forms part of the wetted surface. The flow patterns through a subsonic air inlet at low, design, and high speeds are shown in Figure 1. By maximizing the pressure recovery factor (PR) and bringing it as close to unity as possible, the goal of effective layout of the intake is to reduce fluid losses, as stated in references [5] and [6].

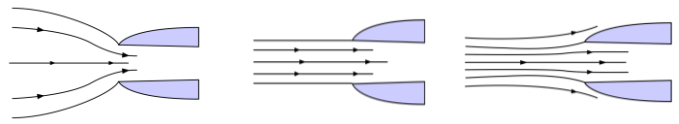

(A) LOW SPEED SUCKING CONDITION. (B) SUBSONIC DESIGN POINT CAPTURE AREA MATCHES INTAKE AREA. (C) HIGH SPEED (SUBSONIC) INTAKE SPILLING.

FIGURE 1: STREAM LINES AT LOW, DESIGN, AND HIGH SPEEDS FOR SUBSONIC INTAKE [5].

A shockwave is created as the free stream flow accelerates close to the nacelle lip as it reaches the engine diffuser at high angles of attack (AOA), [7]. The boundary layer thickens due to the typical nacelle's lower lip shock. If the shock is sufficiently strong, it can induce separation that leads to complete intake separation. Figure 2 illustrates the essential components of intake flow dynamics at high angles of attack, including complete separation, [8]. The performance of the engine intake is affected by different phases of aircraft operation, especially changes in angle of attack (AOA), which in turn influence engine performance, [9].

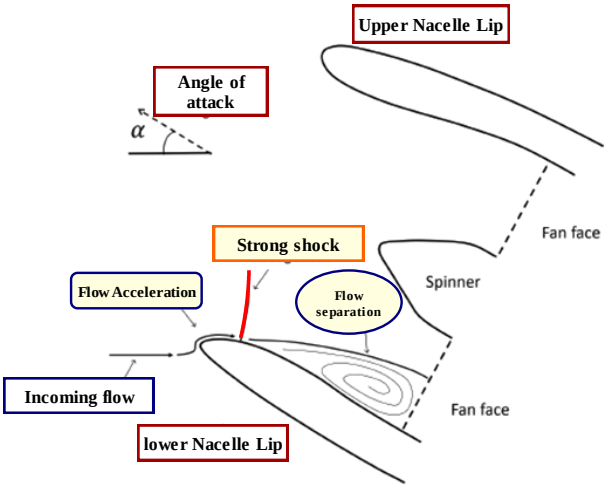

FIGURE ٢: DIAGRAM SHOWING THE PHYSICS OF FLOW NEAR A HIGH-INCIDENCE INTAKE IN A CRITICALLY SEPARATED STATE.

Engine intakes must be designed to be narrower and shorter to address the growing diameter of engine inlets due to higher bypass ratios in future engines. This design strategy also aims to reduce drag and weight. However, the increased diffuser angles of shorter intakes can exacerbate shock-induced

ISSN: 2636 - 3712 (Printed Version)
ISSN: 2636 - 3720 (Online Version)

separation under off-design conditions, [10]. By utilizing an extended modular version of the single-equation model of turbulence, specifically the Spalart–Allmaras model, positive outcomes have been achieved. This progress aids in creating a more reliable intake design framework. The model is used to predict crosswind flow over the intake lip in a 90-degree sector, considering both smooth and rough surface conditions, [11]. Flow separation and reattachment-related hysteresis phenomena are studied, [12]. To validate a subsonic cruise vehicle using empirical data, a commercial CFD code is employed to model the flow field, combining the Navier-Stokes equations with a stable, three-dimensional, density-based one-equation turbulence model, [13]. The goal of ongoing research is to create an intake-compressor system that is inherently more resilient to surge and stall events. By using this method, compressor stall will be prevented without the need for intricate control systems, [14]. It is investigating the S-duct intake's aerodynamic design for subsonic circumstances, [15]. This study considers five length-to-offset ratios and two centering ratios as design criteria. Each configuration is analyzed using CFD simulations at various AOA, and the resulting data is estimated. For each configuration, Recovery coefficients and total pressure distortions are computed.

The thermodynamic cycle of the GE90 engine determines thrust (T) and thrust-specific fuel consumption (TSFC) based on parameters such as bypass ratio (B), overall pressure ratio (OPR), and turbine inlet temperature (TIT), as examined in [16]. The research indicates that thrust increases with turbine inlet temperature (TIT) but decreases with higher bypass ratio (B) and overall pressure ratio (OPR). Conversely, thrust-specific fuel consumption (TSFC) increases with TIT while decreasing with higher B and OPR. Additionally, as noted in [17], climatic factors such as temperature, humidity, and pressure significantly affect the durability and performance of aircraft turbine engines. Additionally, the adverse effects of air pollution are acknowledged as a significant factor in engine degradation. This study primarily focuses on the constraints imposed on airplane takeoff weight (TOW) and the required runway length, which are influenced by varying weather conditions. Research in [18] examines how changes in the anti-icing mass flow rate from a system of bleed air impact performance of the anti-icing system, particularly in high bypass ratio and two-spool turbofan engines.

Building on prior research, this paper investigates the effect of intake performance on high bypass and three-spool turbofan engines across various angles of attack (0, 10, 20, 30, and 40 degrees). Initially, a computational model of the turbofan engine intake is employed to analyze flow parameters at an altitude of 12,000 meters and a Mach number (M) of 0.82 at different angles of attack, using ANSYS FLUENT® 19 and the Spalart-Allmaras model to assess pressure recovery (PR). Subsequently, the thermodynamic cycle of the turbofan engine is examined using MATLAB® software to evaluate the impact of intake performance during various flying phases regarding engine performance. Figure 3 illustrates the outline of the phases involved in this investigation. This study introduces new insights by uncovering how various flight phases influence engine configurations and intake efficiency.

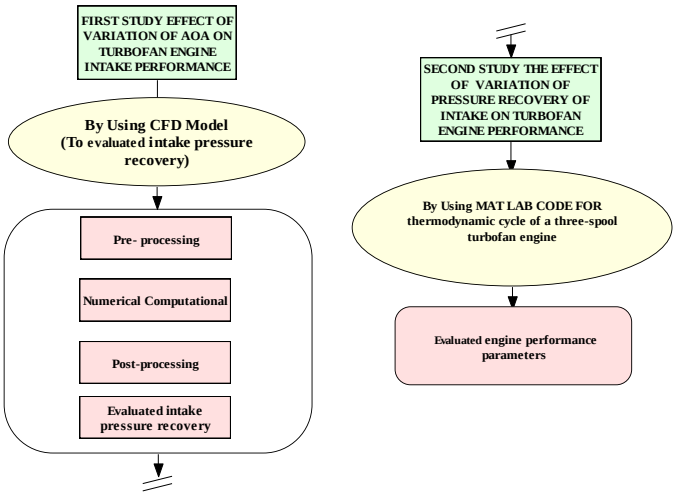

FIGURE 3: AN OUTLINE OF THE PHASES INVOLVED IN THIS INVESTIGATION.

II.EFFET OF VARIATION OF AOA ON TURBOFAN ENGINE INTAKE PERFORMANCE

The primary goal of this research is to expect the intake performance (PR) of a turbofan engine across angles of attack (AOA) ranging from 0 to 40 degrees. While intake performance is traditionally determined through experimental testing, this approach can be time-consuming and more expensive compared to using Computational Fluid Dynamics (CFD). CFD has develop an essential tool for aiding in the development, optimization, innovation, verification, and validation of engineering processes, as noted in [19] and [20].

A. Turbofan Engine Intake Numerical Modeling and Dimensions

This study's flow is regarded as compressible and external-internal. Figure 4 illustrates the geometry of the CFD model for the turbofan engine intake. The dimensions for the front diameter, fan diameter, intake thickness, and hub diameter are 2.205 m, 2.304 m, and 0.6 m, respectively.

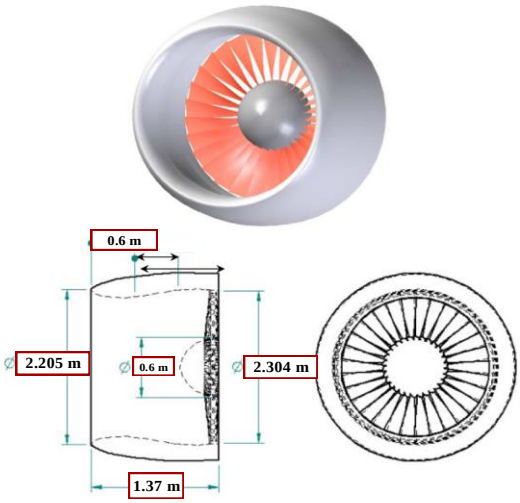

FIGURE 4: TURBOFAN ENGINE INTAKE GEOMETRY.

The boundary conditions defined at the "farfield" boundary include an ambient static temperature of 216.7 K, an ambient static pressure of 19,330.41 Pa, and M of 0.82 at an altitude of

12,000 meters. For the "pressure-outlet" boundary, the entire temperature as well as the ambient static pressure are specified. The "pressure-outlet" boundary is employed in the fan model, allowing for the calculation of the fan face's static pressure to achieve the desired flow rate, effectively simulating the actual mass airflow under specific flight conditions. The hub is adjusted to the average static temperature of the surrounding airflow, and the nacelle is modeled as a wall of constant temperature that maintains the same ambient static temperature as the farfield. Figure 5 illustrates the domain boundary types: hub (wall), pressure outlet (fan), nacelle (wall), and pressure farfield.

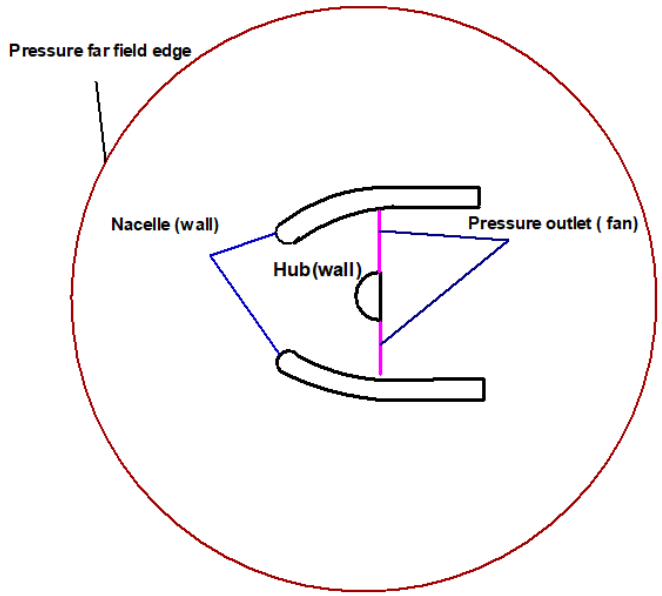

FIGURE 5: A COMPUTATIONAL MODEL OF TURBOFAN ENGINE INTAKE.

B. Turbofan Engine Intake Domain Discretization

The mesh for the study is created using the Mesh tool in ANSYS FLUENT®19. It is crucial to minimize grid size at the boundaries, specifically around the intake and hub walls, to ensure accuracy. To optimize memory usage and reduce computation time, the grid volumes farther from the boundaries are made as large as possible. The mesh employs a size function with a rate of growth of 1.01, a 1 mm maximum grid size, and a 1 mm maximum grid size at the intake and hub walls. The total number of cells is approximately 4.12578×10^5, and the mesh is an unstructured triangle-pave grid. The average skewness quality for each model is around 0.19124, indicating excellent mesh quality, as shown in Figure 6.

C. Check for grid dependencies

A grid independence investigation was conducted to maximize the number of grid cells without sacrificing accuracy. While increasing the number of cells generally enhances the precision of numerical solutions, it also demands more computational resources, including memory and processing time. The ideal mesh is obtained by refining the grid until further increases in cell count no longer affect the results. To assess the results'

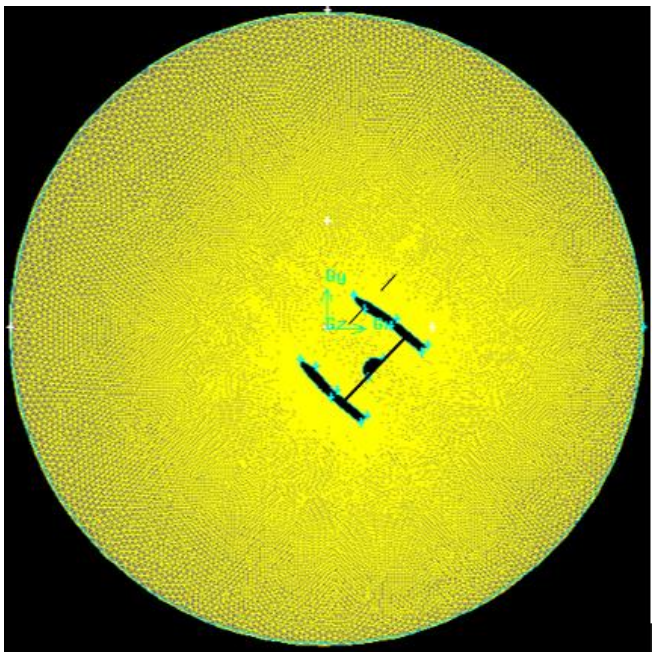

FIGURE 6: AN EXAMINATION IS CONDUCTED ON THE TURBOFAN ENGINE INTAKE'S MESHED CONTROL SURFACE.

independence from the cell count, five different mesh configurations were tested. As a function of the number of cells, Figure 7 displays the distribution of static pressure along the intake length, with an angle of attack of 0 degrees and a Mach number of 0.82.Approximately 4.12578×10^5 cells were determined to be sufficient for reducing solution time without affecting the accuracy of the results. An Intel Core i7 CPU with 16 GB of RAM was used for all computations, and the scaled residual was lowered to a value less than 10^{-6}.

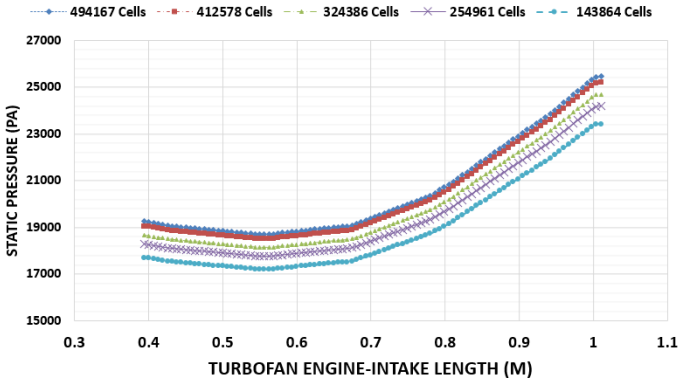

FIGURE 7: STATIC PRESSURE (PA) AT MACH NUMBER OF 0.82 AND AOA OF 0 DEGREES PLOTTED VERSUS THE TURBOFAN ENGINE-INTAKE LENGTH (M) FOR VARIOUS NUMBERS OF GRID CELLS.

III.RESULT AND DISCUSSIONS

The turbofan engine intake is evaluated at different angles of attack (AOAs: 0, 10, 20, 30, and 40 degrees) to assess the effects of AOA on pressure recovery (PR) and overall efficiency at M of 0.82 and an altitude of 12,000 meters. Simulations are conducted using ANSYS FLUENT® 19 CFD software, utilizing the Spalart-Allmaras turbulence model to analyze intake performance.

A. Velocity vectors around turbofan engine intake

The airflow properties delivered by the intake play a significant role in engine performance, making efficient inlets a critical component of any propulsion system. Intake design and operation directly affect air compression, flow stability, and pressure recovery, all of which are essential for optimizing engine performance. As depicted in Figure 8-a, the velocity vector at an AOA of 0 degrees shows no signs of flow separation, indicating minimal losses and an increase in pressure recovery (PR). In contrast, Figure 8-b illustrates the velocity vector at an AOA of 40 degrees, where flow separation occurs, leading to turbulence, energy dissipation, and a reduction in pressure recovery. Ensuring stable and attached airflow through the intake is crucial for maximizing pressure recovery and minimizing losses, which is a key consideration in propulsion system design.

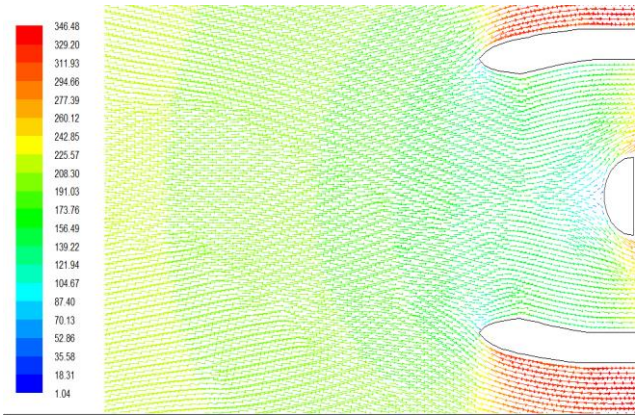

a) TURBOFAN ENGINE INTAKE WITH AOA 0 DEGREE.

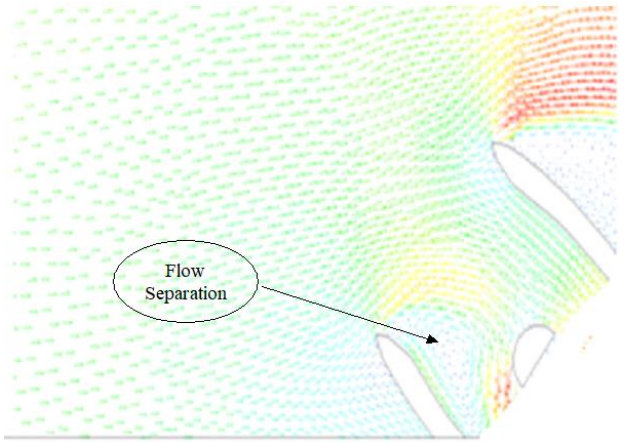

b) TURBOFAN ENGINE INTAKE WITH AOA 40 DEGREE.

FIGURE 8: TURBOFAN ENGINE-INTAKE SURFACE VELOCITY VECTOR (M/S) WITH M OF 0.82 AND ALTITUDE OF 12000 M.

B. Velocity magnitude and static pressure along turbofan engine intake

Pressure recovery can decrease due to several factors, including turbulence caused by flow separation and losses resulting from boundary layer effects on the diffuser walls. As previously mentioned, an increase in AOA leads to greater losses within the intake and a corresponding reduction in pressure recovery. The primary function of an inlet in a propulsion system is to increase the pressure of incoming airflow, as shown in Figure 9-b. This is achieved by slowing the flow velocity, as depicted in Figure 9-a. Under compressible flow conditions, the inlet effectively operates as a compressor. At an AOA of 0 degrees, the pressure recovery reaches approximately 0.98, indicating highly efficient inlet performance. However, at an AOA of 40 degrees, pressure recovery drops to around 0.92, highlighting a significant decline in performance due to flow separation and increased losses at the higher angle of attack.

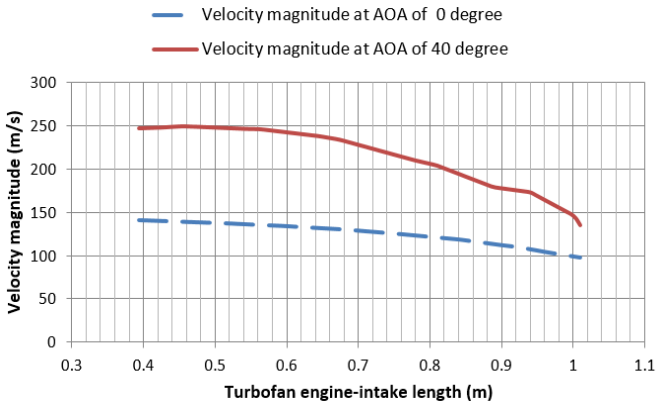

a) VELOCITY MAGNITUDE WITH AOA OF 0 AND 40 DEGREE.

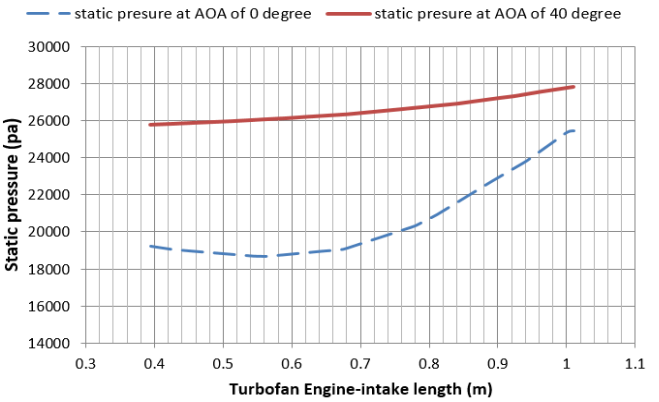

b) STATIC PRESSURE WITH AOA OF 0 AND 40 DEGREE.

FIGURE 9: VELOCITY MAGNITUDE (M/S) AND STATIC PRESSURE (PA) AS AFFECTED BY TURBOFAN ENGINE-INTAKE (M=0.82, AT ALTITUDE=12000 M).

IV. EFFECT OF VARIATION OF PRESSURE RECOVERY OF INTAKE ON TURBOFAN ENGINE PERFORMANCE

In order to analyze the thermodynamic cycle of a three-spool turbofan engine, such as the TRENT 1000, the incoming airflow is separated into hot and cold streams. After passing through the fan, the cold stream exits through the fan nozzle. As shown in Figure 10, the engine consists of three spools: the high-pressure turbine drives the compressor on the high-pressure spool, the low-pressure turbine powers the fan on the low-pressure spool, and the intermediate-pressure turbine drives the compressor on the intermediate-pressure spool.
Figure 11 shows the engine arrangement, including the states of the three-spool turbofan engine and the T-S diagram. Assume that the properties upstream and downstream of the combustion chamber are constant, with (ɣc, Cpc) for the upstream and (ɣh, Cph) for the downstream.

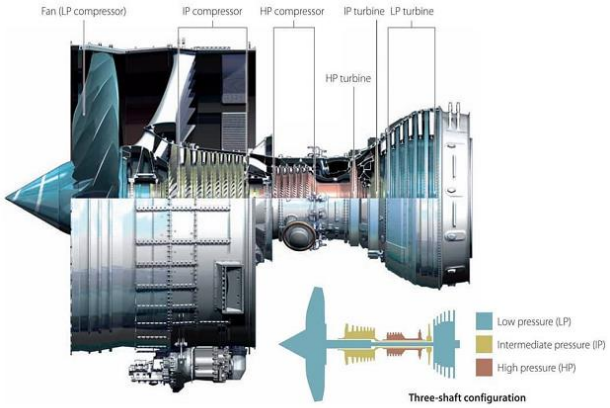

a) A THREE SPOOL TURBOFAN ENGINE LIKE (TRENT 1000)

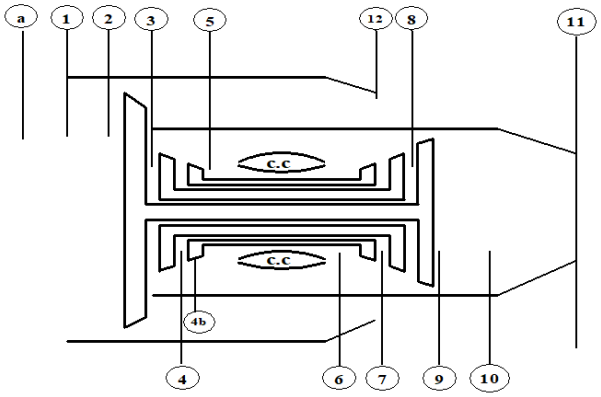

b) ENGINE LAYOUT WITH STATES OF THERMODYNAMIC CYCLE

FIGURE 10: A THREE SPOOL TURBOFAN ENGINE LIKE (TRENT 1000) AND ENGINE LAYOUT WITH STATES OF THERMODYNAMIC CYCLE.

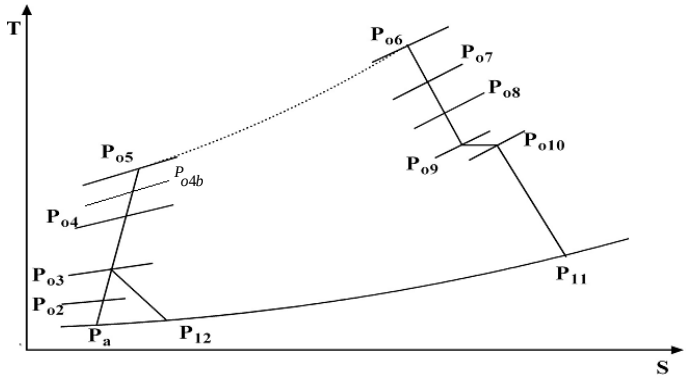

FIGURE 11: SCHEMATIC DIAGRAM FOR A T-S ENGINE, A THREE-SPOOL TURBOFAN.

A. *Three-spool turbofan engine thermodynamic cycle analysis*

Thermodynamic process equations were applied to all of the engine's components as follows:
The engine intake pressure recovery (PR) can be described as follows:

$$P_{oa} = P_a\left(1+\frac{\gamma_c-1}{2}M_a^2\right)^{\gamma_c/\gamma_c-1}$$

$$P_{o2} = P_{oa}\times\pi_{pr}\text{, where } \pi_{pr} \text{ is pressure recovary factor} \rightarrow(1)$$

$$T_{o2} = T_a\left(1+\frac{\gamma_c-1}{2}M_a^2\right) \rightarrow(2)$$

Intake PR is taken between 0.92 and 0.98 in the CFD intake model used in the study. The equation describing the performance parameters for three-spool turbofan engines are as follows:

- *specific thrust:*

$$\frac{T}{m_a^\circ} = \left[\left(\frac{1}{1+\beta}\right)\left[\begin{array}{l}(1+f)\times V_{11}+\beta\times V_{12}+(1+f)\left(\frac{RT_{11}}{PV_{11}}\right)\left(P_{11}-P_a\right)\\ +\beta\left(\frac{RT_{12}}{PV_{12}}\right)\left(P_{12}-P_a\right)\end{array}\right]-V\right] \rightarrow(3)$$

Where: T is the thrust force, m_a° is the air mass flow rate, V is the flight speed, V11 is the exhaust hot gases speed, and V12 is the exhaust cooled gases speed.

- *Thrust specific fuel consumption (TSFC):*

$$TSFC = \frac{f/(1+\beta)}{T/m_a^\circ} \rightarrow(4)$$

- *Propulsive: efficiency:*

$$\eta_p = \frac{T/m_a^\circ\times V}{T/m_a^\circ\times V+\left[0.5\left(\frac{1+f}{1+\beta}\right)(V_{11}-V)^2\right]+\left[0.5\left(\frac{\beta}{1+\beta}\right)(V_{12}-V)^2\right]} \rightarrow(5)$$

- *Thermal efficiency:*

$$\eta_{th} = \frac{T/m_a^\circ\times V+\left[0.5\left(\frac{1+f}{1+\beta}\right)(V_{11}-V)^2\right]+\left[0.5\left(\frac{\beta}{1+\beta}\right)(V_{12}-V)^2\right]}{\left(\frac{f}{1+\beta}\right)Q_R} \rightarrow(6)$$

- *Overall efficiency:*

$$\eta_o = \eta_p\times\eta_{th} = \frac{T/m_a^\circ\times V}{\left(\frac{f}{1+\beta}\right)Q_R} \rightarrow(7)$$

The primary goal of this software is to ascertain the connections between engine design parameters (such as pressure recovery of the intake, compressor pressure ratio, fan pressure ratio, bypass ratio, etc.) and engine performance (Such as specific fuel consumption (TSFC), thrust T, etc.). Constraints associated with the flight environment (like the M, ambient temperature, ambient pressure, etc.) include the burner exit temperature and compressor exit pressure. Next, the effect of varying intake pressure recovery (PR) on engine performance is assessed. To evaluate the impact of intake pressure recovery on engine performance, the thermal cycle of a three-spool turbofan engine is simulated and analyzed using MATLAB 7 software. Table 1 presents the design characteristics and operating circumstances with a range of variation for the case study of a three-spool

turbofan engine, such as the Trent 1000. The Trent 1000 engine design parameters and operating conditions are reported in [21], and [22].

TABLE 1: A THREE-SPOOL TURBOFAN ENGINE'S OPERATING CONDITIONS

properties	value	properties	value	properties	value
π_{pr}	[0.92 : 0.99]	λ_3	1	π_{IPC}	5.8
η_f	0.9	M	0.82[0.2:0.85]	π_{HPC}	4.2
η_c	0.89	π_F	1.45	γ_c	1.4
η_b	0.98	$TIT\ (K)$	1543	γ_h	1.33
η_t	0.93	$\Delta p_{c.c}$	0.03		
η_n	0.98	$\Delta p_{fan\,duct}$	0		
η_m	0.99	$cp_c\,(J/kg.K)$	1005		
λ_1	0.84	$cp_h\,(J/kg.K)$	1148		
λ_2	1	$R(J/kg.K)$	287		

B. Result and discussion of three spool turbofan engine performance analysis.

For verification of three spool turbofan engine MATLAB code, the variations of engine performance with selected thermodynamics parameters changes such as Mach number (M) is investigated on Figure 12. The difference in particular thrust as a function of pressure recovery factor and Mach number. At a constant Mach number, Figure 12 illustrates that the specific thrust increases with enhancing pressure recovery factor. The specific thrust rises by about 4% when the pressure recovery factor is raised from 0.92 to 0.99.

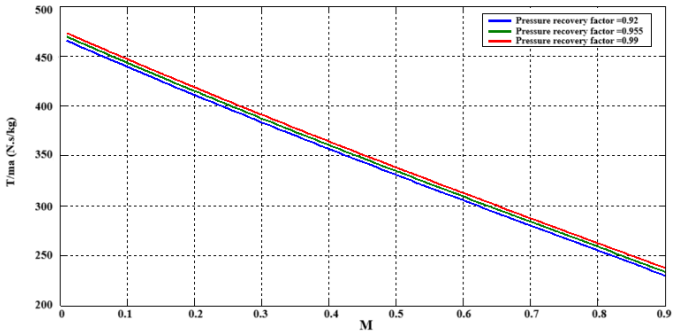

FIGURE 12: DISTRIBUTION OF SPECIFIC THRUST (T/m_a°) FOR THREE SPOOL TURBOFAN ENGINE WITH (M).

Figure 13 depicts the changes in thrust-specific fuel consumption (TSFC) in response to variations in M and PR factor. At a constant M, an increase in the PR factor leads to a decrease in TSFC. Specifically, raising the PR factor from 0.92 to 0.99 results in an approximate 3% reduction in TSFC.

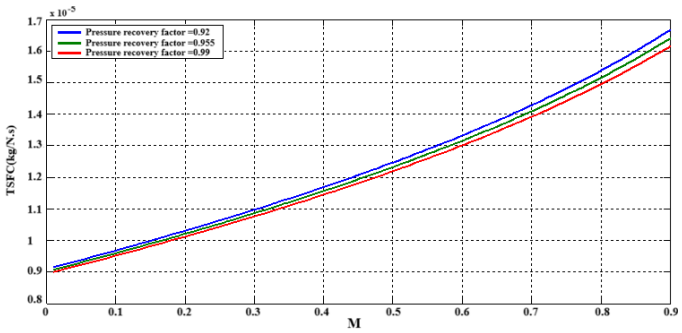

FIGURE 13: DISTRIBUTION OF THRUST SPECIFIC FUEL CONSUMPTION ($TSFC$) FOR THREE SPOOL TURBOFAN ENGINE WITH (M).

The difference in thermal efficiency brought about by adjustments to the PR factor and M is examined in Figure 14. Figure 14 shows that thermal efficiency (η_{th}) increases at a constant M as the PR factor rises. Thermal efficiency (η_{th}) increases by about 2.5% when the PR factor is raised from 0.92 to 0.99.

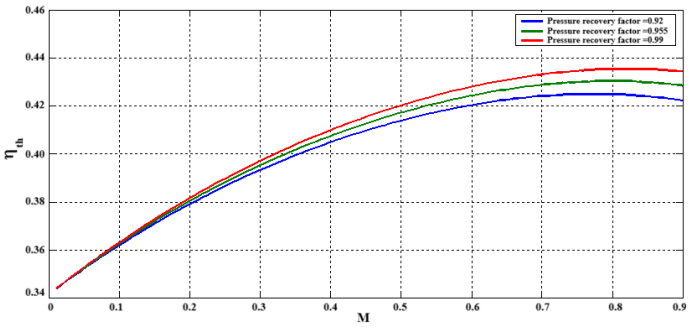

FIGURE 14: DISTRIBUTION OF THERMAL EFFICIENCY (η_{th}) FOR THREE SPOOL TURBOFAN ENGINE WITH (M).

The variation of propulsive efficiency (η_p) as a function of PR factor and M is examined from Figure 15. Figure 15 illustrates how propulsive efficiency (η_p) increases at a constant M as the PR factor improves. The propulsive efficiency (η_p) rises by roughly 2% when PR factor is increased from 0.92 to 0.99.

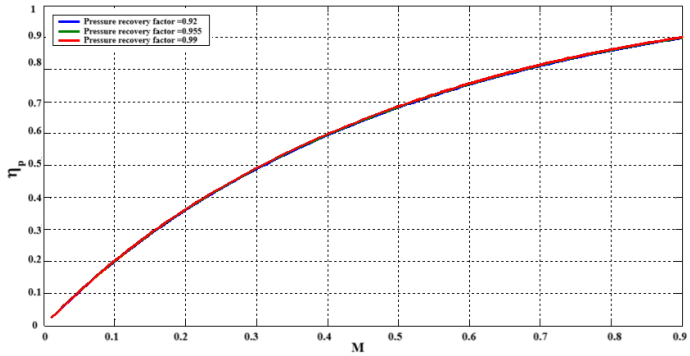

FIGURE 15: DISTRIBUTION OF THERMAL EFFICIENCY (η_p) FOR THREE SPOOL TURBOFAN ENGINE WITH (M).

The variation of overall efficiency (η_o) as a function of PR factor and M is examined from Figure 16. Figure 16 illustrates how overall efficiency (η_o) improves at fixed M as the PR factor rises. The overall efficiency (η_o) improves by roughly 4% when PR factor is increased from 0.92 to 0.99.

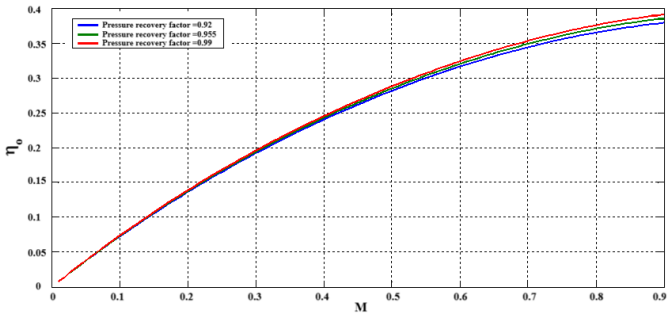

FIGURE 16: DISTRIBUTION IN THE THREE-SPOOL TURBOFAN ENGINE'S OVERALL EFFICIENCY (η_o) WITH (M).

V.CONCLUSIONS

The turbofan engine intake efficiency (pressure recovery) in aircraft is very important to enhance the engine performance. From first study, it is investigated a CFD Model of turbofan engine intake with various angle of attack (40, 30, 20, 10, and 0) degrees to evaluate the pressure recovery on engine intake. The main results showed that the pressure recovery of engine intake decreased with increasing the angle of attack. Specifically, at an AOA of 0 degrees, the pressure recovery is approximately 0.98, indicating a highly efficient inlet operation. In contrast, at an AOA of 40 degrees, the pressure recovery drops to around 0.92, demonstrating a significant deterioration in performance due to the flow separation and increased losses at the higher angle of attack.

Using MATLAB software, the second study examines the thermodynamic cycle of a three-spool turbofan engine. The engine's performance parameter with Mach number changed from 0 to 0.9 is demonstrated with varying engine intake pressure recovery values ranging from 0.92 to 0.99. The findings are summed up as follows:

- Raising pressure recovery (PR) from 0.92 to 0.99, which results in an approximate 4% rise in average specific thrust with Mach number changed from 0 to 0.9.
- The average thrust-specific fuel consumption (TSFC) was reduced by approximately 3%.
- The average propulsive efficiency was enhanced by approximately 2%.
- The average thermal efficiency was enhanced by approximately 2.5%.
- The average overall efficiency was enhanced by approximately 4%.

Finally, it is shown that pressure recovery in the engine intake should be enhanced during all phases of flight to minimize any negative impact on engine performance.

VI.REFERENCES

[1]- S. Kallas, M. Geoghegan-Quinn, M. Darecki, C. Edelstenne, T. Enders, et al, “Flightpath 2050 Europe’s vision for aviation”. Report of the high level group on aviation research. Brussels, Belgium: European commission, Report No. EUR 98, (2011).

[2]- Teng Cao, Nagabhushana Rao Vadlamani, Paul G Tucker, Angus R Smith, Michal Slaby, and Christopher TJ Sheaf. Fan-intake interaction under high incidence. Journal of Engineering for Gas Turbines and Power, 139(4):041204, 2017.

[3]- Essam E. Khalil, Eslam AbdelGhany, Mahmoud A. Fouad and Ahmed El-Sayed. Effect of Pressure Recovery on Triple Spool Turbofan Engine Performance, 11th International Energy Conversion Engineering Conference, July 14 - 17, 2013, San Jose, CA, https://doi.org/10.2514/6.2013-3926.

[4]- Sijian Tan and Dimitri Mavris. CFD Validation of Engine Inlet Duct Pressure Loss Model for Subsonic Non-Uniform Cross-Section Duct, AIAA 2024-3918 Session: Aerodynamics of Inlets and Nozzles Published Online:27 Jul 2024, https://doi.org/10.2514/6.2024-3918.

[5]- A.F. El-Sayed, “Aircraft Propulsion and Gas Turbine Engines” CRC Press, 2008.

[6]- J.D. Mattingly, “Elements of Propulsion: Gas Turbines and Rockets” AIAA Education Series, 2006.

[7]- Robert Christie, Alexander Heidebrecht, and David MacManus. An automated approach to nacelle parameterization using intuitive class shape transformation curves. Journal of Engineering for Gas Turbines and Power, 139(6):062601, 2017, DOI: 10.1115/1.4035283.

[8]- J. Alistair, B. James, Q. Ning, “Using shock control bumps to improve engine intake performance and operability.” The Aeronautical Journal, Page 1 of 35, 2019, doi: 10.1017/aer.2020, https://eprints.whiterose.ac.uk/170561/.

[9]- Essam E. Khalil, Eslam AbdelGhany, Mahmoud A. Fouad, and Ahmed El-Sayed. “Effect of Pressure Recovery on Triple Spool Turbofan Engine Performance”. AIAA 2013-3926, https://doi.org/10.2514/6.2013-3926.

[10]- A. Kozakiewicz, M. Frant, M. Majcher, “Impact of the intake vortex on the stability of the turbine jet engine intake system”. International Review of Aerospace Engineering. 2021; 14: 173–180, DOI: 10.15866/irease.v14i4.20223.

[11]- Ugochukwu R. Oriji, Paul G. Tucker. “Modular Turbulence Modeling Applied to an Engine Intake” J. Turbomach. May 2014, 136(5): 051004 (10 pages), https://doi.org/10.1115/1.4025232.

[12]- Cesare A Hall and Thomas P Hynes. Measurements of intake separation hysteresis in a model fan and nacelle rig. Journal of Propulsion and Power, 22(4):872–879, 2006, DOI: 10.2514/1.18644.

[13]- T. V., Yogesh, Nidamarty, Laasya Priya, S. V., Ramanamurthy and Panigrahi, S. K.. "Design and analysis of air intake of subsonic cruise vehicle with experimental validation" International Journal of Turbo & Jet-Engines, 2024. https://doi.org/10.1515/tjj-2024-0007.

[14]- K. Adam, A. Maciej, W. Mirosław, Areas of Investigation into Air Intake Systems for the Impact on Compressor Performance Stability in Aircraft Turbine Engines., Advances in Science and Technology Research Journal 2022, 16(1), 62–74, htt ps://doi.org/10.12913/22998624/143290.

[15]- K. Jayaprakash, S. Kandasamy, G. Debkumar, and C. Girish Varma, “Aerodynamic Design and Numerical Analysis of S-Duct Intake.” ICETE 2023, AER 223, pp. 1226–1233, 2023, https://doi.org/10.2991/978-94-6463-252-1_123.

[16]- B. Shray, and W. Jiqiang, “Dynamic Modeling and Simulation on GE90 Engine”. The International Journal Of Engineering And Science (IJES), Volume 5, Issue 12, Pages PP 111-119, 2016.

[17]- Włodzimierz BALICKI, Paweł GŁOWACKI, Stefan SZCZECINSKI, Ryszard CHACHURSKI, Jerzy SZCZECIŃSKI, “EFFECT OF THE ATMOSPHERE ON THE PERFORMANCES OF AVIATION TURBINE ENGINES”., acta mechanica et automatica, vol.8 no.2 (2014), DOI 10.2478/ama-2014-0012.

[18]- E.S. Abdelghany, H.H. Sarhan, A. El Saleh, Mohamed B. Farghaly, High bypass turbofan engine and anti-icing system performance: Mass flow rate of anti-icing bleed air system effect, Case Studies in Thermal Engineering, Volume 45, 2023, 102927, ISSN 2214-157X, https://doi.org/10.1016/j.csite.2023.102927.

[19]- E. S. Abdelghany, Khalil, E. E., O. E. Abdelatif, and G. M. ElHarriry, “COMPUTATIONAL ANALYSES OF AERODYNAMIC

CHARACTERISTICS OF NACA653218airfoil". Proceedings, AIAA paper AIAA_2016_1_ 2307246, https://doi.org/10.2514/6.2016-1367.

[20]- E.S. Abdelghany,; E.E. Khalil,; O.E Abdellatif,.; G. ElHarriri,Winglet Cant and Sweep Angles Effect on Aircraft Wing Performance. In Proceedings of the 17th International Conference on Applied Mechanics and Mechanical Engineering, Cairo, Egypt, 19–21 April 2016; Military Technical College, Kobry El-Kobbah: Cairo, Egypt, 2016; Volume 17, pp. 1–17, DOI: 10.21608/amme.2016.35282

[21]- Essam E. Khalil, Gamal A. ElHarriri, Eslam S. AbdelGhany and Mohamed Hussien. A Proposed Triple Stream Turbofan New Engine. 2018 AIAA Aerospace Sciences Meeting 8–12 January 2018, Kissimmee, Florida, https://doi.org/10.2514/6.2018-2256.

[22]- Abdelghany ES, Ahmed F. El-Sayed, Mahmoud A. Fouad and Essam E. Khalil,"Effect of Film colling of HP and IP turbines on Performance of triple Spool Turbofan Engines," Jul. 2012;30:1-3, DOI: 10.2514/6.2012-3988.

VII. NOMENCLATURE

- **List of symbols**

A_{ec}	Exit area for the cold stream
A_{eh}	Exit area for the hot stream
b1	Turbine cooling Bleed air ratio $\left(m^{\circ}_{turbine\ bleed} / m^{\circ}_{a}\right)$
b2	Anti-icing Bleed air ratio $\left(m^{\circ}_{Anti-icing\ bleed} / m^{\circ}_{a}\right)$
C_{pc}	Specific heat of cold air
C_{ph}	Specific heat of hot air
f	Fuel to air ratio
M_a	Mach number
$\overset{\circ}{m}_a$	Total air mass flow rate in engine, (kg/sec) $(\overset{\circ}{m}_h + \overset{\circ}{m}_c)$
$\overset{\circ}{m}_c$	Air mass flow passing through the fan (kg/sec)
$\overset{\circ}{m}_h$	Air mass flow passing through the hot section of engine (kg/sec)
p	Pressure (N/m2)
P_{ec}	Exhaust pressure of the cold stream
P_{eh}	Exhaust pressure of the hot stream
ΔP_{cc}	Pressure drop in combustion chamber
$\Delta P_{fan\,duct}$	Fan duct pressure drop
ΔP_{mix}	Mixer pressure drop
Q_R	Fuel heating value
T	Thrust (N)
T / m°_{a}	Specific thrust (N.s/kg)
u_{ec}	Velocity of cold air leaving the fan nozzle
u_{eh}	Velocity of hot gases leaving the turbine nozzle
V	flight speed (m/sec)

- **Greek Letters**

β	By bass ratio, $m^{\circ}_{c} / m^{\circ}_{h}$
γ_c	Specific heat ratio of cold air
γ_h	Specific heat ratio of hot air
η_d	The diffuser isentropic efficiency
η_f	Fan isentropic efficiency
η_{HPC}	High compressor isentropic efficiency
$\eta_{H.p.t}$	High turbine isentropic efficiency
η_{IPC}	Intermediate Compressor isentropic efficiency
η_{IPT}	Intermediate turbine isentropic efficiency
$\eta_{L.p.t}$	Low turbine isentropic efficiency
η_n	Nozzle isentropic efficiency
η_o	Overall efficiency, $\eta_o = \eta_{th} \times \eta_p$
η_p	Propulsive efficiency
η_{th}	Thermal efficiency
π_f	Fan pressure ratio
π_{HPC}	High compressor pressure ratio
π_{IPC}	Intermediate compressor pressure ratio

- **List of Abbreviations**

AI-BAS	Anti-icing bleed air system
HBPT	High by pass turbofan
HPC	High pressure compressor
PSM	Partial span model
TIT	Turbine inlet temperature